Intensification of Tropical Cyclone FANI Observed by INSAT-3DR Rapid Scan Data

Neeru Jaiswal
Space Applications Centre, ISRO
Sanjib K. Deb (sanjib_deb@rediffmail.com)
Space Applications Centre, ISRO
Chandra M. Kishtawal
Space Applications Centre, ISRO

Research Article

Keywords: Tropical cyclone, remote sensing, INSAT 3DR, rapid scan operation, satellite, cyclone eye.

Posted Date: August 30th, 2021

DOI: https://doi.org/10.21203/rs.3.rs-368454/v1

Version of Record: A version of this preprint was published at Theoretical and Applied Climatology on February 8th, 2022. See the published version at https://doi.org/10.1007/s00704-022-03957-1.

Abstract

Geo-stationary satellite images are one of the primary tool for real-time monitoring and intensity analysis of Tropical Cyclones (TCs) in spite of other complimentary remote sensing sensors like scatterometers, microwave imagers and sounders, mounted on the polar orbiting satellites. The weather activities over Indian region are continuously monitored by two Indian geostationary satellites viz., INSAT-3D and INSAT-3DR for every 15 minutes in staggered mode. During extreme weather events like TCs, INSAT-3DR is operated in rapid scan operation mode by taking observations over the system in every 4-minutes interval. These observations are highly useful in understating the instantaneous structural changes during evolution, intensification and landfall of TC. The salient observations over the cloud systems by visible, thermal infrared (TIR1), and water vapour imageries of INSAT-3DR satellite during the life cycle of the TC FANI are presented in this paper. The rapidly evolving small-scale features inside the inner core of TC FANI in high temporal resolution images were examined. The large-scale circulation features are analysed by atmospheric motion winds generated using rapid scan infrared images of INSAT-3DR. The relationship between TC intensity and inner core TIR1 BT, number of overshooting top clouds in the differenced TIR1-WV BT have been presented by analysing the sequence of INSAT-3DR imageries. The strong correlation (r^2=0.74) was obtained between the TC eye temperature and radial distance of first overshooting cloud top. The 1 km x 1 km visible images of TC were found to have the presence of small-scale mesovortices in the eye region, which are a typical characteristic of intense TC system. The rapid scan operation mode generated sequence of images have been presented to show their application to identify the signatures of TC intensification.

1. Introduction

The rapid scan images from geostationary satellites have been proven to be useful tools in weather applications like the derivation of atmospheric motion winds, analysis of wildfires, convective initiation nowcasting, and identification of overshooting convective cloud tops (Schmidt et al., 2014; Bedka et al., 2015; Line et al., 2016; Mohapatra et al., 2021). These images are useful for monitoring the convective features of storms that evolve on shorter time scales i.e. less than 15 or 30-minutes (Dworak et al. 2012; Cintineo et al. 2013). Several unique signatures have been identified within satellite imagery of severe convective storm tops, which include rapid cloud-top cooling (Cintineo et al. 2013), overshooting tops (Dworak et al. 2012), above-anvil cirrus plumes (Levizzani and Setvák 1996), the cold ring (Setvák et al. 2010) etc. Bedke et al., 2015 have shown the relationships between the different properties of deep convective storms observed by high temporal resolution satellite imageries and radar. One-minute interval images of GOES-12 have been used to feature the mesovortices inside the eye of tropical cyclone (Kossin and Schubert, 2004).

Tropical cyclones are the weather event with complex multi-scale processes and non-linear interactions. The temporal frequency of satellite-generated images is critical for extreme weather events like TCs because significant changes in the atmosphere during a short interval are possible (Sun et al., 2019). Moreover, the spatial resolution of the imaging system determines the detail of the observed textures,

which is very important for fine-scale target tracking. Researchers have shown that convective scale processes within the hurricane core might have played a crucial role in influencing rapid changes in TC intensity and structure (Rogers, 2010). The strong relationship between the satellite measured BT of cloud tops near the core of TCs and its current and future intensity has been well-demonstrated (Gentry et al. 1980; Dvorak, 1975). Past observational studies have documented that intensifying TCs have outflow that links to synoptic scale upper tropospheric flow features, while non-intensifying TCs have no such link. Outflow tends to develop in regions where upper tropospheric inertial stability is low and stronger outflow tends to be associated with intensifying TCs. The data provided by geostationary satellites in high temporal sampling mode may give insight into the upper level outflow and rapidly changing structural features of TCs, which may be used as a guidance of TC intensification processes. The satellite-derived features of inner core can be used as an indicator of TC rapid intensification (Callaghan et al., 2017). In the past few years, due to the advance developments in in-situ and satellite based measurements, there has been some drastic improvements in the TC inner core observations. The observations from the advanced sensors like GPS dropsonde, step frequency microwave radiometer (SFMR), aircraft reconnaissance, weather radar systems, satellite microwave sensors, radiometers, sounders, rapid-scan satellite imagers, scatterometers etc. have provided huge amount of data for studying the TC inner core dynamics (Kepert, 2010).

India's two meteorological geostationary satellites viz., INSAT3D and INSAT3DR provides coverage over India and surrounding regions including the oceans. INSAT-3D and INSAT-3DR both have two meteorological payloads, an Imager (with 6 channels) and a Sounder (with 18 infrared channels and a visible channel for daytime cloud detection). The Imager has capability of taking observations of full earth-disk from geostationary orbit in one visible channel (VIS, 0.55–0.75 μm) and five infrared (IR) channels: Shortwave infrared (SWIR, 1.55–170 μm), Midwave infrared (MIR, 3.8-4.0 μm), Water Vapor absorption channel (WV, 6.5–7.1 μm), and two split-window thermal infrared channels (TIR1,10.2–11.2μm and TIR2,11.5 to12.5 μm). The observations from VIS and SWIR channels are available at 1 km x 1 km ground resolution at nadir, whereas MIR, TIR1, and TIR2 has resolution of 4 km x 4 km. The WV channel has coarser resolution of 8 km x 8 km at nadir. The sub-satellite points of INSAT3D and INSAT3DR are at 82^0 E and 74^0 E, respectively.

The Indian geostationary satellite INSAT3DR is being operated in rapid scan operation mode during high impact weather activities like TCs to capture the images in every 4-minutes interval. These satellite observations may be helpful in observing the rapidly changing features over TCs and thus determining its movement, structure and intensity. The atmospheric motion winds generated using rapid scan images during tropical cyclone time shows potential for providing very good quality winds information over Indian Ocean by increasing the amount of wind data availability and by capturing atmospheric movement that are too short-lived to be depicted by routine 30-minute scans. During the extremely severe TC FANI, in the Bay of Bengal during 26 April-04 May 2019, the INSAT3DR satellite was operated in rapid scan mode. This TC was developed near the equator, which is very rare, and made landfall at the Odisha coast after achieving extremely severe tropical cyclone category. The present work aims to discuss the

fine scale short-lived features within TC i.e. eye-eyewall mesovortices, double eyewall, over shooting cloud top etc. and its association with TC intensification. The visual animation of TIR1, WV, visible and differenced “TIR1-WV” imageries over TC were also extensively analysed to observe the deep convective cloud-top movement, out flow characteristics and other structural features. The pattern of large-scale circulation around the cyclone is also analysed by using atmospheric motion winds in rapid scan mode.

1.1. Overview of Tropical cyclone FANI (26 April – 03 May 2019)

The TC “FANI”, was classified by India meteorological department (IMD) as extremely severe cyclonic storm. It was originated from a tropical depression formed at west of Sumatra in the North Indian Ocean on 26 April 2019. Vertical wind shear at first hindered the storm's development, but conditions became more favourable on 30 April. TC FANI rapidly intensified into an extremely severe cyclonic storm and reached its peak intensity on 02 May, as a high-end extremely severe cyclonic storm, and the equivalent of a high-end Category 4 major hurricane on Saffir simpson scale. FANI made landfall as extremely severe cyclone category on 03 May morning hours and its convective structure rapidly degraded thereafter, dissipating on 05 May. Prior to its landfall, authorities in India and Bangladesh evacuated at least a million people each from FANI's predicted path onto higher ground and into cyclone shelters, which is thought to have reduced the resultant death toll. The real-time observed cyclone track from Joint typhoon warning center (JTWC) have been shown in the Fig. 1. The cyclone category based on its intensity is also shown in the figure.

2. Data Used And Methodology

The INSAT-3DR satellite data during the evolution and active period of TC FANI i.e. 26 April-04 May 2019 have been used in the present work. During this period, satellite was scanning in the Rapid Scan Operation mode, with satellite images produced in 4 and 9 minutes interval. Gridded satellite data obtained in the present work have been taken from MOSDAC server. The best track data of TC FANI used in the study have been obtained from the Joint Typhoon Warning Centre (JTWC) and Regional Specialized Meteorological Centre (RSMC) for tropical cyclones over North Indian Ocean, India Meteorological Department (IMD), Delhi. During the active period of TC FANI, INSAT-3DR was operated in rapid scan operation mode by taking observations over the system in every 4-minute interval. The present study includes all the observations by INSAT-3DR over TC FANI during 29 April – 03 May 2019. This includes the different intensity stages of TC from cyclonic storm to extremely severe cyclonic storm category. The histogram of intensity of stages of TC FANI observed by INSAT-3DR are shown in the Fig. 2. Out of total 971 satellite observations, 74 (7.6%) were made over cyclonic storm stage (34–47 knots), 147 (15.2%, SCS) over severe cyclonic storm intensity stage (48–63 knots), 192 (19.8%, VSCS) over very severe cyclonic storm intensity stage (64–85 knots), 558 (57.5%, ESCS) over extremely severe cyclonic storm intensity stage (86–119 knots). IMD cyclone intensification classification has been used in this study. IMD provides 3-hourly best track data and JTWC provide 6-hourly best track data. Cooperative

institute of meteorological satellite studies (CIMSS) provides the half-hourly intensity estimation using Advanced Dvorak Technique (ADT), which have been used in the present work. For rapid scan (4-minute interval) images the intensity values were obtained from the interpolation of half hourly ADT intensity estimates of CIMSS.

The present study includes visual analysis of images of tropical cyclone FANI generated from the high scanning rate (~ 4 minutes) data captured by imager channels of INSAT-3DR satellite. The short-lived features (< 15 minutes) observed by visible, TIR1 and water vapour (WV) channel data have been discussed in this study. The differenced images of TIR1 and WV channel were also analysed to examine the overshooting clouds and its association with tropical cyclone intensification.

3. Results And Discussions

3.1 TC FANI observed by INSAT-3DR TIR1 Imageries

The visual animation of TIR1 imageries over TC were monitored to observe the deep convective cloud-top movement over TC at high-temporal resolution by INSAT-3DR satellite. The 4 km spatial resolution TIR1 imageries were analysed to identify the short-lived features and its association with TC intensity. The images shows a well-defined eye with an annular to axisymmetric eyewall structure. A blow up of convection can be clearly seen near the center of circulation. A sample image of TC FANI by TIR1 channel at 1515 UTC 02 May 2019 has been shown in the Fig. 3. The color enhanced image is also presented. The red shades in the colour enhanced image represent the area with regions colder than − 30 ^{0}C grading through to white color, which represents area colder than − 70 ^{0}C. The warm eye can be seen in the images with temperature greater than + 10 ^{0}C.

All the archived TIR1 images of TC over open ocean areas with eye conditions during 01 May-02 May 2019 were examined for the warmest TIR1 BT in the eye of TC. The time series plot of BT in TC eye and corresponding intensity has been shown in the Fig. 4. TIR1 BT in the eye of TC is found increasing with the increasing intensity values. Thus, the higher values of TIR1 BT in TC eye can be used as an indicator of TC intensification. The warmest temperature in eye of TC by TIR1 channels was observed as 293.78 K on 1232 UTC 02 May 2019. During this hour TC achieved its peak intensity of 115 knots and was categorised as an extremeley severe TC as per the IMD intensity classification criterion.

The variability of TIR1 BT in the inner core of TC during its intensification was investigated by computing the standard deviation of TIR1 BT. The TIR1 observed BT values of the inner core region i.e. area within 2 degrees from TC center was used to compute the standard deviation in each image. The center of the cyclone was manually identified for each image by identifying the warmest pixel in the center of circulation. The TIR1 BT standard deviation (STD) was then plotted with the corresponsding intensity of TC as showin in Fig. 5. The STD values were found to be decreasing during intensification of TC. The values of STD was minimum during high intensity stages. The minimum value of inner core TIR1 STD was found as 9.51 K during its peak intensity of 115 knots.

3.2 TC FANI observed by INSAT-3DR differenced TIR1-WV Imageries

The WV spectral response peak is about 350 mb, whereas the IR peak is at or near the surface. Due to this weighting function characteristic, during clear sky conditions the TIR1 BT is always warmer than WV BT values as TIR1 BT represents temperature near surface and WV BT represents temperature above the surface. However, during the presence of deep clouds the weighting functions shifts further and the BT measured by WV becomes warmer than IR. The pixels with warmer WV BT than IR shows the deep convective clouds. Thus, in opaque cloud conditions associated with intense active convection penetrating the tropopause, the sign of the measured difference between the two channels can reverse due to the reemitted absorbed radiation from upper-tropospheric–lower-stratospheric (UTLS) water vapor (Schmetz et al. 1997). The sequence of differenced TIR1-WV BT images for TC FANI have been generated and analysed for the existence of any short-lived features during TC life period.

One of the sample image representing INSAT-3DR observed TIR1, WV and differenced (TIR1-WV) BT of TC FANI during 1453 UTC 02 May 2019 has been shown in the Fig. 6. The distinguishable, warm and intense eye can be seen in the given image for both the channels. One can see that eye temperature observed in TIR1 is warmer than the WV channel, this reflects the presence of clear eye with low levels or no clouds. In the differenced image the BT in eye region is positive and has been shown in white colour. However, the negative BT of grreater than 20 degrees can be seen in the inner core region of TC surrounding eye area, near the eye-wall region.

The differenced BT (IR-WV) values of two channels during the entire life of cyclone was computed and analysed. To minimize the size of paper the images during 0758–0853 UTC 01 May 2019 have been shown in the Fig. 7. These images well represents the asymmetric clouds within eyewall and inner core region of TC. The presence of over shooting clouds at some locations is found rapidly changing as it alters in the next 4 minute imageries. The deep overshooting clouds (blue in colour, with differenced BT $<-20^0$C) were observed in the southern part of the eyewall whereas the low clouds (red in colour, with differenced BT close to 0 ^{0}C) were present in the norther part. The extent of differenced BT was found to be changing in every 4 minute images.

The correlations between the total number of negative pixels in inner core region of TC and its current and future intensity was further investigated. The time series plot of number of negative TIR1-WV pivels in TC inner core region and intensity has been shown in the Fig. 8. Figure shows that there is a lag between the number of negative pixels and the intensity changes. This result can be utilised to address the future intensification of TC.

3.3 Rapid scan atmospheric motion winds as observed from INSAT-3DR satellite

The atmospheric motion winds generated using rapid scan infrared images of INSAT-3DR data are analysed in this section. Since the time interval between rapid scan images are shorter, the winds derived using rapid scan images will be able to capture small-scale circulation features better than normal winds derived using 30-minute images. TC FANI rapidly intensified into an extremely severe cyclonic storm and reached its peak intensity on 02 May 2019, and the scan areas of rapid scan images were modified as per the location of cyclonic storm. The steps of wind derivation algorithm for rapid scan mode is same as that of operational algorithm (Deb et al. 2016), however, because of higher temporal resolution in rapid scan small changes are incorporated in the algorithm in respect to tracer size selection and tracking time steps. In this study atmospheric motion winds generated using rapid scan images of 01 May 2019 of INSAT-3DR satellite are analysed and qualitative comparison are shown using operationally available INSAT-3D winds. The Fig. 9 shows the temporally nearest INSAT-3D winds valid at 0200 UTC (Fig. 9a) and 0230 UTC (Fig. 9b) for 01 May 2019 using normal 30-minute images. In the figure, red colour box indicates the approximate coverage area of rapid scan from INSAT-3DR satellite. The Fig. 10 shows the typical examples of rapid scan atmospheric motion winds derived over the Indian Ocean region [30^{o}E – 130^{o}E, 2^{o}N – 20^{o}N] using TIR-1 channel of INSAT-3DR in rapid scan mode valid at 0158 UTC (Fig. 10a), 0206 UTC (Fig. 10b), 0219 UTC (Fig. 10c) and 0228 UTC (Fig. 10d) on 01 May, 2019. It is observed from the zoomed version of Figs. 9(a1, b1) and Fig. 10(a1, b1, c1, d1) that the large-scale features near cyclone are captured very well and high density wind vectors are generated near tropical cyclone centre in rapid scan mode using INSAT-3DR satellite, when compared with normal 30-minute retrieval using INSAT-3D satellite. The higher temporal resolution in rapid-scan mode enables improved tracking of cloud motions and which in turn generates a dense wind flow pattern during a tropical cyclone. These rapid scan winds can provide very useful information for operational forecaster, for assimilating these in the numerical model.

3.4 TC eyewall mesovortices observed in the visible images of INSAT-3DR satellite

The visible imageries of 1 km x 1km resolution of TC FANI was analysed to identify some characteristics features. The TC FANI observed by INSAT3DR visible wavelength during its peak intensity stage at 0802 UTC (left) and 0945 UTC (right) 02 May 2019 has been shown in the Fig. 11.

In the eyewall of intense tropical cyclones, tornado scale rotational features i.e. mesovorices have been speculated since last two decades. Due to their small hoizontal scale, fast movement and associated severe turbulence, it is often found difficult to observe them directly (Wu et al., 2018). In these vortices wind speed can be upto 10% higher than in the rest of eyewall. These are the characterics features of intense TCs typically observed during the periods of intensification.

The numerical simulations of hurricane models run at a horozontal grid spacing of 2–3 km have been demonstrated the occurrence of mesovortices or small scale cores of rotating deep clouds (called as vortical hot towers) (Montogomery et al., 2006; Hendricks et al., 2004; Hendricks et al., 2006). These

features within the eye of intense TC have also been reported from the visible images from the rapid scan high spatial resolution observations of other geostationary satellites like visible imageries (0.64 μm) of Himawari-8 satellite for typhoon Jebi (30 AUG 2018) and 1-minute GOES-16 visible data for hurricane Florence (11 September 2018), GOES-15 visible data for hurricane Hector (06 August 2018). The animation of visible images (I km resolution) obtained from INSAT-3DR rapid scan provide the signatures of transient low-level cloud swirls in eye of TC FANI during its intensification stage on 01–02 May. These small scale regions of vorticity are known as mesovortices and their presence in TC eye and eyewall are widely documented (Kossin et al., 2002). The visible image of INSAT3DR showing the mesovortices (yellow circled) and hot towers (red circles) is given in Fig. 11.

The closer look of the inner core of TC FANI taken from 1 km resolution visible imageries of INSAT-3DR during the period 0800–1000 UTC 02 May 2019 have been presented in Fig. 13. These visible channel images shows a distinct eye and eyewall with the surface mesovortices features within the eye of TC. In every 4 minute images these features of multiple mesovortices was found rapidly evolving and dissipating. The moat of clear air at the edge of eye represents strong subsidence (Schubert et al., 2007). These observations along with the numerical simulations can give better insight of TC intensification. The details of eye structure in-terms of its temperature, size and shape may also be helpful in TC intensity estimation.

3.5 Radial location of First overshooting top (FOT)

TC core has been defined as a region within 200 km from TC center. Radial location of the first overshooting top (FOT) was identified using “TIR-WV” BT differences. The FOT was determined by locating the radial point closest to the TC Center (i.e. minimum radial distance) where a negative “TIR-WV” BT difference was found at any azimuthal direction. The relation between radial distance of first over shooting top and pressure drop at eye was investigated by plotting the scatter diagram between FOT and TIR BT of TC eye. The scatter plot has been presented in the Fig. 14. It can be seen from the figure that there has been a strong correlation (R^2 = 0.74) between TIR BT of TC eye and FOT. This was computed for only clear eye cases (317) during 01 May-02 May 2019. This shows that as the temperature in eye is increasing the size of eye is also expanding resulting in the increased values of FOT.

During the analysis, the warmest TIR1 BT was found at 1232 UTC 02 May 2019 for TC FANI, before its landfall. The inner core of TC has been shown during this hour in Fig. 15. The 40 km diameter eye can be observed during this time. The diameter of eye in this case is approximated by the positive number of “TIR1-WV” differenced BT image pixels in the center of circulation. The TIR-WV BT representing increasing FOT during TC intensification has been shown in the Fig. 16. The expanding size of TC eye can also be visualized in the TIR-WV differenced BT values.

4. Conclusions And Future Work

TCs formed in the North Indian Ocean are monitored by geostationary satellites viz., INSAT-3D and INSAT3DR in addition to the polar satellite based microwave instruments like scatterometer (SCATSAT) and humidity sounder (SAPHIR). During active TC period in NIO, INSAT-3DR satellite is operated in rapid scan mode, providing data over TC latitudes in every 4-minutes. This data has been utilized in this work to address the structural changes in inner core of TC FANI during its intensification.

The rapid scan data from INSAT 3DR imager channels i.e. TIR1, WV, visible and differenced “TIR1-WV” was analysed to investigate the fine scale short-lived features within TC. The BT measured by TIR1 channel in the eye of TC was examined and found to be maximum (293.78 K) during its peak intensity. The increasing BT in the eye of TC was a good indicator of TC intensification. The TC inner core mean TIR1 BT and standard deviation as also analysed and its found minimum as 9.51 K during peak intensity value. The 4 km x 4 km differenced images of “TIR1-WV” BT were examined and a systematic lag of approximately 12 hours was found between the number of negative pixels and the intensity changes. These images were found very useful to identify the short lived changes in the TC asymmetric eyewall cloud structure and can be utilised to address the intensification of TC. These images were further utilised to examine the relation between radial distance of first over shooting top from TC center and TIR1 BT in TC eye. Results show a strong correlation (R^2 = 0.74) between TIR1 BT in eye and radial distance of first overshooting cloud top from TC center. The large-scale circulation features around TC is captured quite well when atmospheric motion winds derived using rapid scan TIR1 images are analysed. The 1 km x 1 km resolution visible channel images of INSAT3DR were investigated to identify the rapidly evolving and dissipating surface mesovortices features within the eye of the TC. These mesovortices are the characteristic features of intense TCs, which are typically observed during the periods of intensification. The rapid scan images from INSAT-3DR provides insight into fine scale TC structure, which can be utilized in the real-time to track the system in every 4 minutes and for the guidance of TC intensification.

TC observation, analysis and prediction has improved significantly due to advancements of observations (in-situ, satellite and radar), computational systems and numerical models. The further way forward is to include the artificial intelligence based advanced emerging technologies in addition to the development of more advanced satellite sensors to observe the 3-d structure of convective systems.

5. Declarations

Acknowledgements

The authors are thankful to the Director, Space Applications Centre (ISRO), Ahmedabad and the Deputy Director of EPSA, SAC-ISRO. The authors acknowledge the Joint Typhoon Warning Centre (JTWC) and Regional Specialized Meteorological Centre (RSMC) for tropical cyclones over North Indian Ocean, India Meteorological Department (IMD), Delhi for providing real time cyclone track through their websites. The satellite observations of INSAT-3D, and INSAT-3DR were obtained from MOSDAC (www.mosdac.gov.in).

Code availability: The analysis of results used for the current study are available from the corresponding author upon reasonable request.

Author's contribution: NJ conceived the idea and performed maximum computations. NJ and SKD analysed the results from the computations and wrote the manuscript. CMK added his expertise in the analysed results and overhauled it in the present form.

Funding: No external funding is involved in this study.

Data availability: The satellite data used in this study are available at www.mosdac.gov.in.

Ethics approval: All procedures performed in this study involving human participants were in accordance with the ethical standards of the institution.

Consent to participate: All authors are mutually agreed for communicating this manuscript in the present form.

Consent for publication: All authors give consent for publication of this manuscript at Theoretical and Applied Climatology upon successful completion of review process.

Conflict of interest: The authors declare that there is no conflict of interest.

6. References

1. Bedka K. M., Wang C., Rogers R., Feltz W. and Kanak J., 2015: Examining Deep Convective Cloud Evolution Using Total Lightning, WSR-88D, and GOES-14 Super Rapid Scan Datasets. Weather and Forecasting, Vol., 30, pp. 571-590.
2. Cintineo M. J., Pavolonis J., Sieglaff M., and Heidinger A. K., 2013: Evolution of severe and nonsevere convection inferred from GOES-derived cloud properties. J. Appl. Meteor. Climatol., vol. 52, 2009–2023.
3. Callaghan J., 2017: Asymmetric inner core convection leading to Tropical cyclone intensification. Tropical Cyclone Research and Review, Vol. 6(3-4), 55-66.
4. Deb S. K, Kishtawal C. M, Kumar Prashant, Kiran Kumar A. S., Pal P. K., Kaushik Nitesh and Sangar Ghansham, 2016: Atmospheric Motion Vectors from INSAT-3D: Initial quality assessment and its impact on track forecast of cyclonic storm NANAUK. Atmospheric Research 169:1-16
5. Dvorak, V. R., 1975: Tropical cyclone intensity analysis and forecasting from satellite imagery. Monthly Weather Review, Vol. 103, 420-430.
6. Dworak, R., Bedka K. M., Brunner J., and Feltz W., 2012: Comparison between GOES-12 overshooting top detections, WSR-88D radar reflectivity, and severe storm reports. Weather and Forecasting, Vol. 27, 684–699.

7. Gentry R. C., Rodgers E., Steranka J., Shenk W., 1980: Predicting tropical cyclone intensity using satellite measured equivalent black body temperatures of cloud tops. Monthly Weather Review, Vol. 108, 445-455.
8. Hendricks, E. A., M. T. Montgomery, and C. A. Davis, 2004: On the role of “vortical” hot towers in formation of Tropical Cyclone Diana (1984). J. Atmos. Sci., 61, 1209–1232.
9. Hendricks, E. A., M. T. Montgomery, 2006: Rapid Scan Views of Convectively Generated Mesovortices in Sheared Tropical Cyclone Gustav (2002). Weather and Forecasting, 21, 1041–1050.
10. Kossin, J. P, and Schubert W.H., 2004: Observations: Mesovortices in Hurricane Isabel, Bull. Amer. Meteor. Soc., Vol. 85, 151-153.
11. Kossin, J. P, McNoldy B.D., and Schubert W.H., 2002: Vortical swirls in hurricane eye clouds. Monthly Weather Review, Vol. 130, 3144-3149.
12. Kepert J D., 2010. Tropical cyclone structure and dynamics: Global Perspectives on Tropical cyclones: from science to mitigation, 3-53.
13. Levizzani, V., and Setvák M., 1996: Multispectral, high-resolution satellite observations of plumes on top of convective storms. J. Atmos. Sci., Vol. 53, 361–369.
14. Line W.E., Schmidt T.J., Lindsey D.T., Goodman S.J., 2016: Use of Geostationary Super rapid scan satellite imagery by the storm predictor center, Weather and Forecasting, Vol. 31, 483-494.
15. Mohapatra M, Mitra A. K., Singh Virendra, Mukherjee S. K., Navrial Kavita, Prashar Vikram, Tyagi Ashish, Verma Atul Kumar, Devi Sunitha, Prasad V. S., Ramesh Mudumba and Raj Kumar, 2021: INSAT-3DR-rapid scan operations for weather monitoring over India, Current Science, 120 (6), 1026-1034
16. Montogomery M.T., Nicholls M., Cram T., and Saunders A., 2006: A “vortical” hot tower route to tropical cyclogenesis. J. Atmos. Sci., 63, 355–386., 2006;
17. Schmidt and Co-authors, 2014: GOES-14 Super Rapid Scan Operations to prepare for GOES-R. J. Appl. Remote Sens., Vol. 7, 073462.
18. Schmetz J., Tjembs S. A., Gube M., Berg V. d., 1997: Monitoring deep convection and convective overshooting with Meteosat. Advanced Space Research, Vol., 19, 433-441.
19. Schubert W.H., Rozoff C. M., Vigh J. L., McNoldy B.D., Kossin J. P., 2007: On the distribution of subsidence in the hurricane eye. Q.J. R. Meteorol. Soc., Vol. 133, 595-605.
20. Setvák, M., and Co-authors, 2010: Satellite-observed cold-ring shaped features atop deep convective clouds. Atmos. Res., Vol. 97, 80–96.
21. Sun F., Min M., Qin D., Wang F., Hi J., 2019: Refined Typhoon geometric center derived from high-spatiotemporal resolution geostationary satellite imaging system. IEEE GRSL, Vol., 16 (4), pp. 4999-503.
22. Wu L., Liu Q., and Li Y., 2018: Prevalence of tornado-scale vortices in the tropical cyclone eyewall. Proceedings of the national Academy of Sciences of the United States of America, Vol., 115 (33), 8307-8310.

Figures

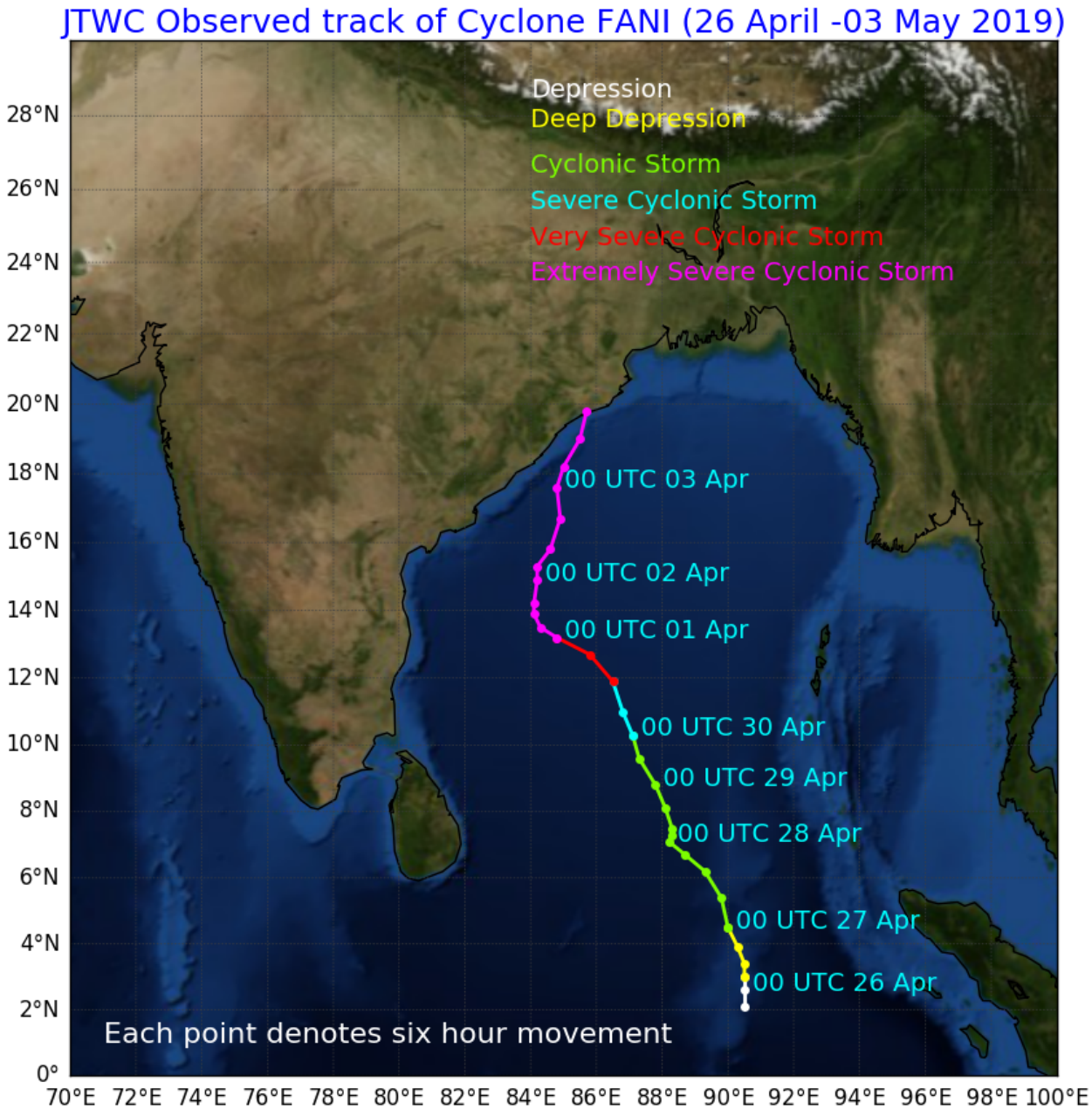

Figure 1

Real-time observed track (JTWC) of TC FANI with its intensity categories.

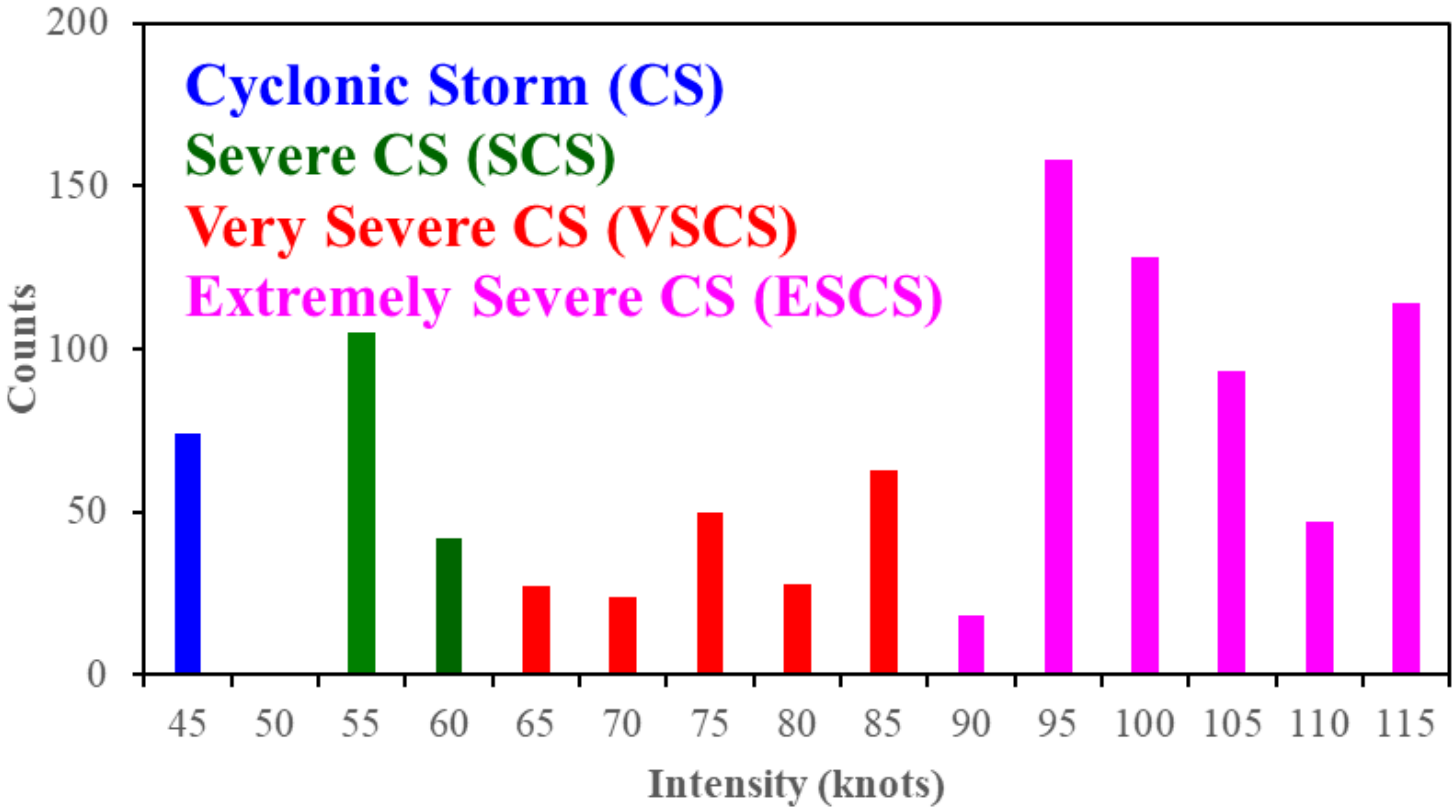

Figure 2

Histogram of intensity associated with the scenes of TC FANI provided by INSAT-3DR during 29 April -02 May 2019.

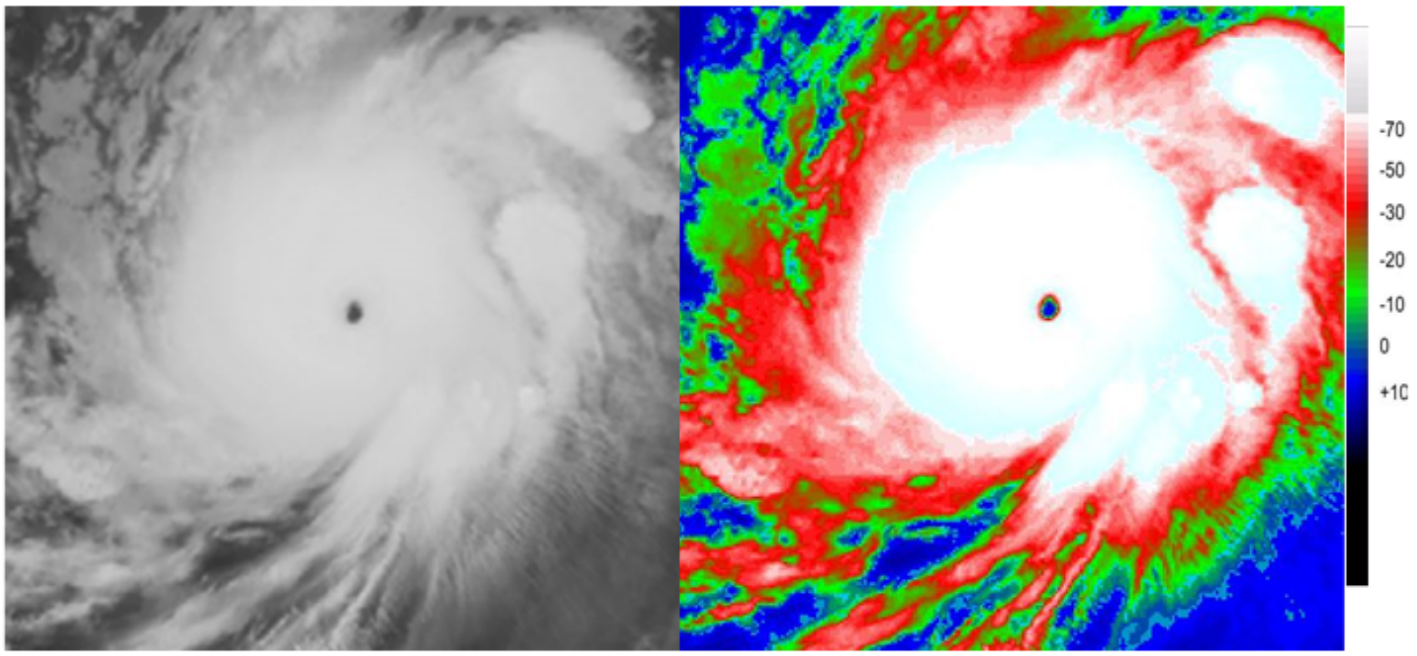

Figure 3

TIR1 image of TC FANI at 1515 UTC 02 May 2019. The color enhanced image (right) with red area making regions colder than -30 0C grading through to white colder than -70 0C.

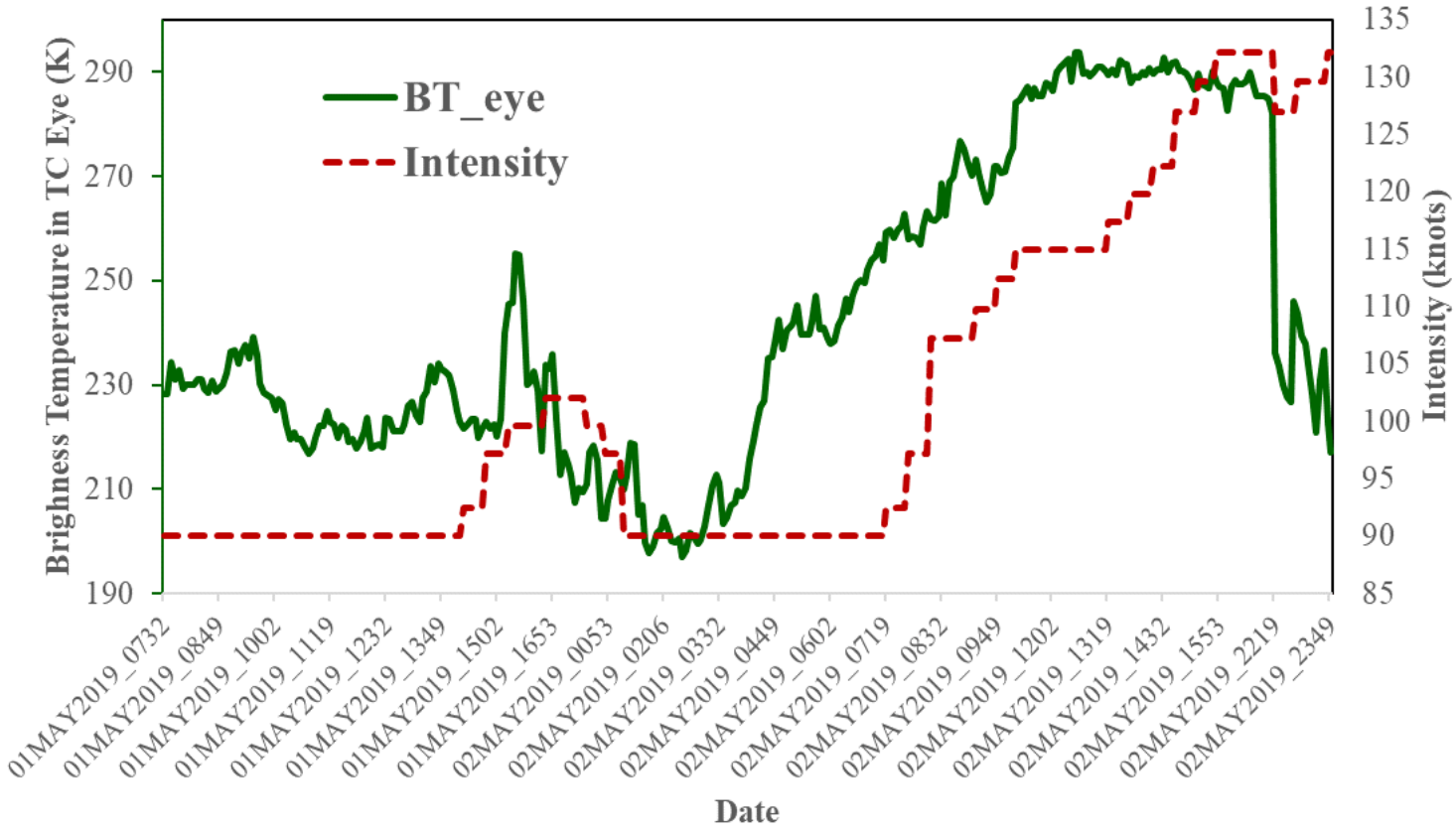

Figure 4

The time series plot of TIR-1 BT in TC eye and intensity

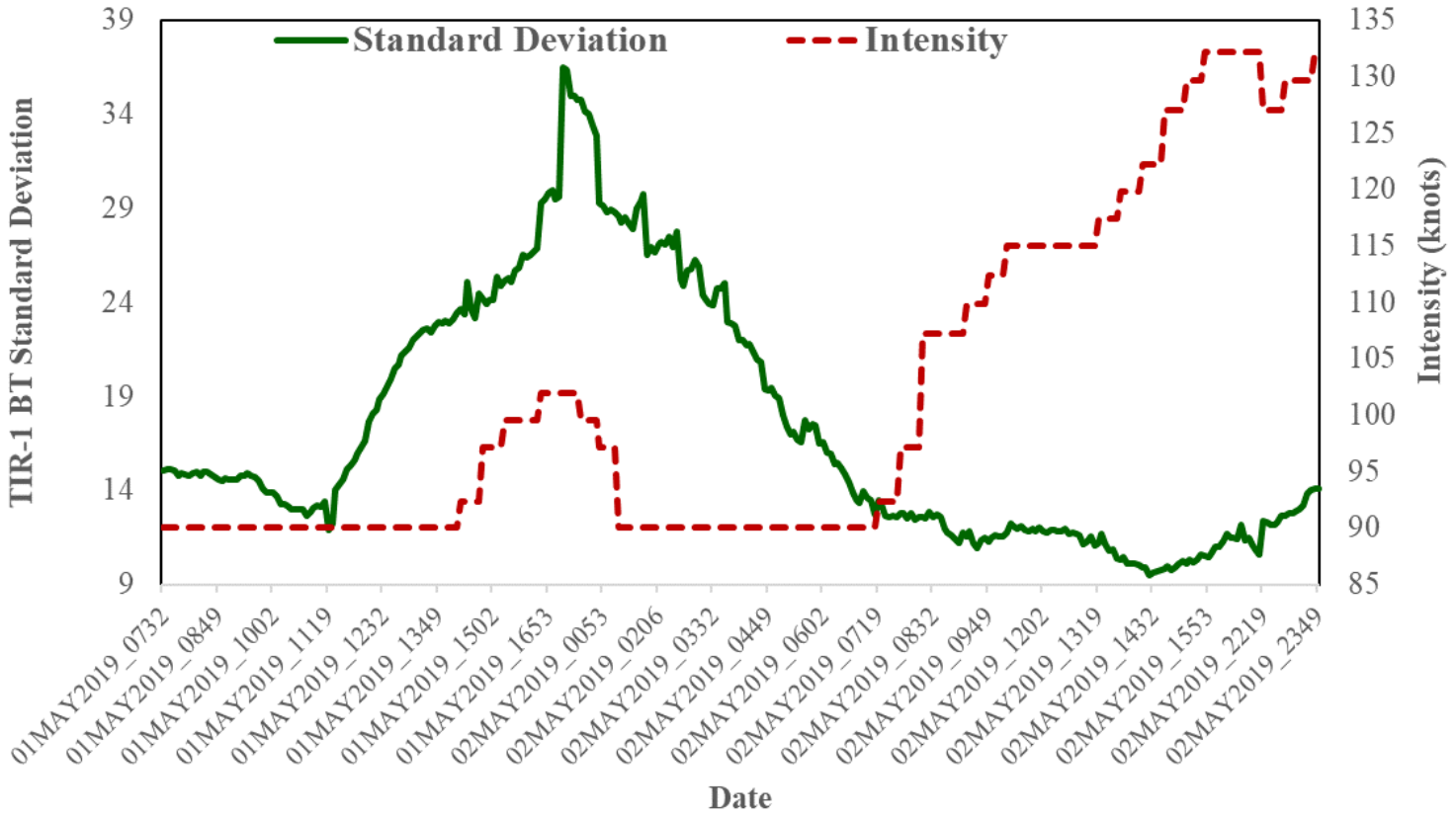

Figure 5

The time series plot of TIR-1 BT standard deviation in TC inner core region and intensity

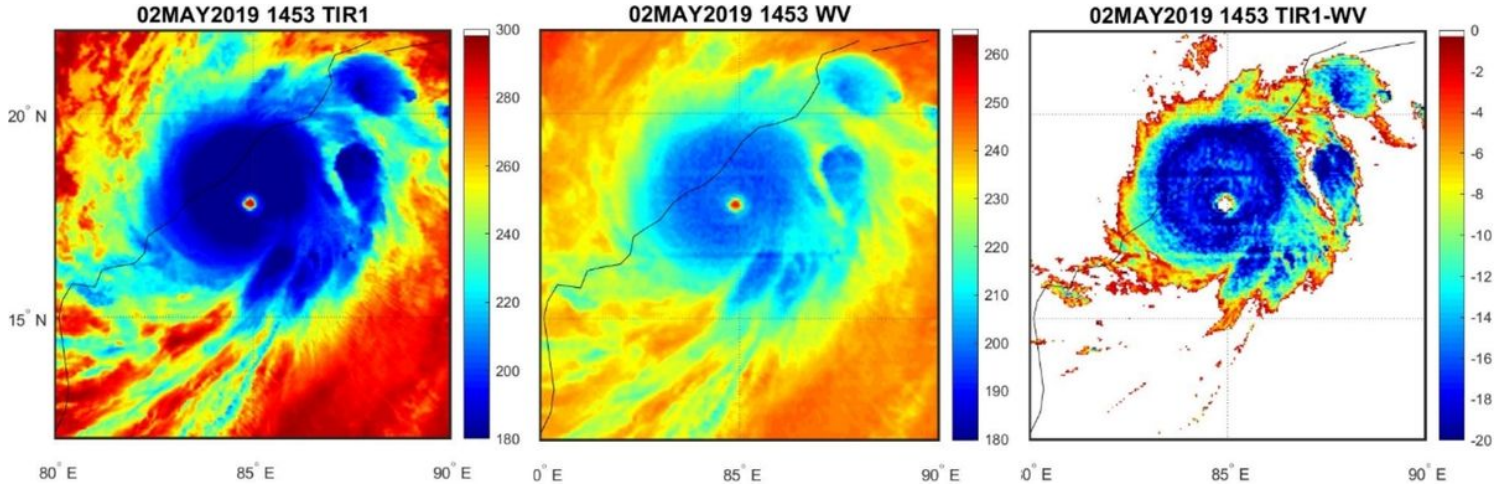

Figure 6

INSAT-3DR observed TIR1, WV and differenced (TIR1-WV) imaregries of TC FANI during 1453 UTC 02 May 2019.

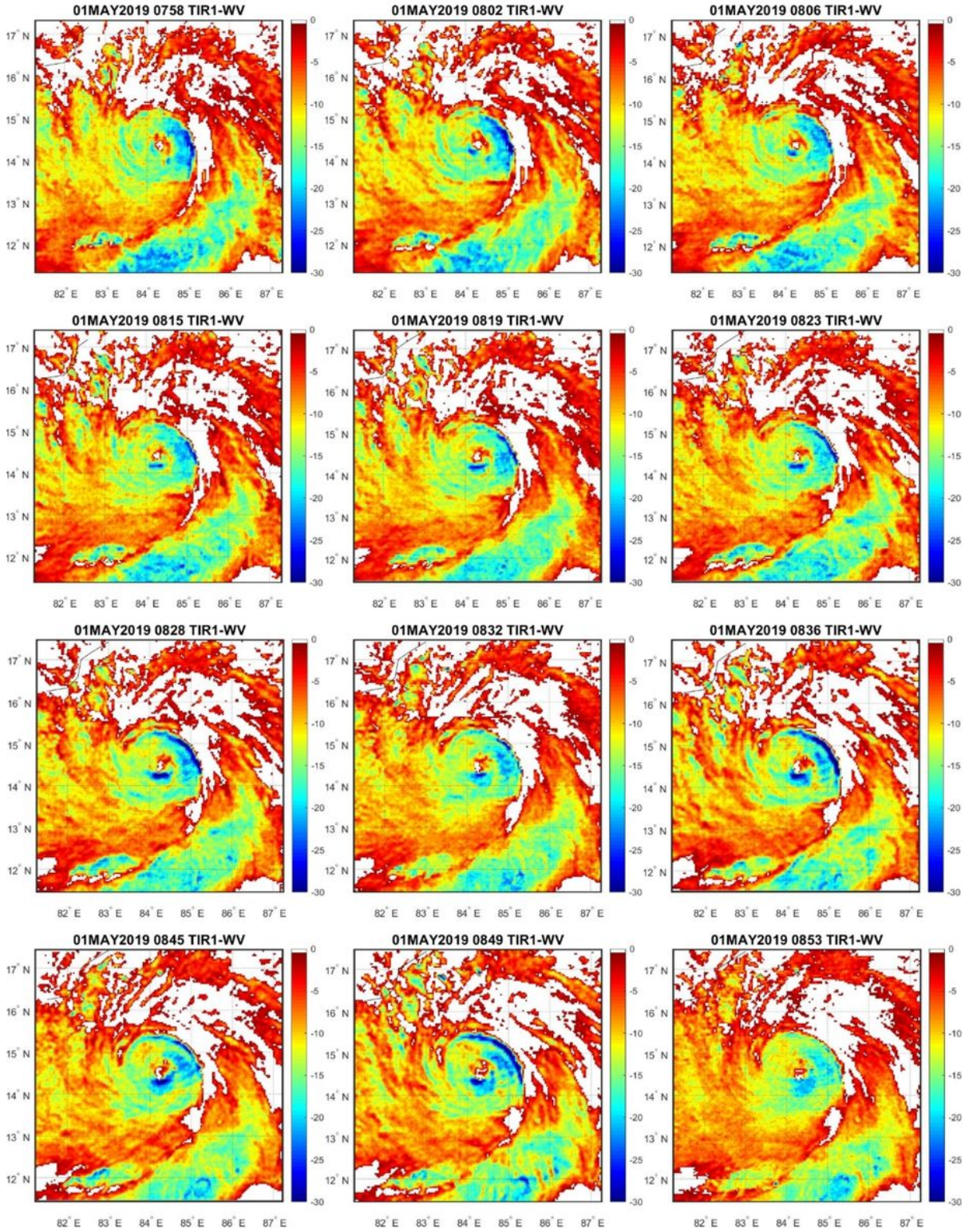

Figure 7

Asymmetric clouds within eyewall and inner core region of TC FANI during 0758-0853 UTC 01 May 2019.

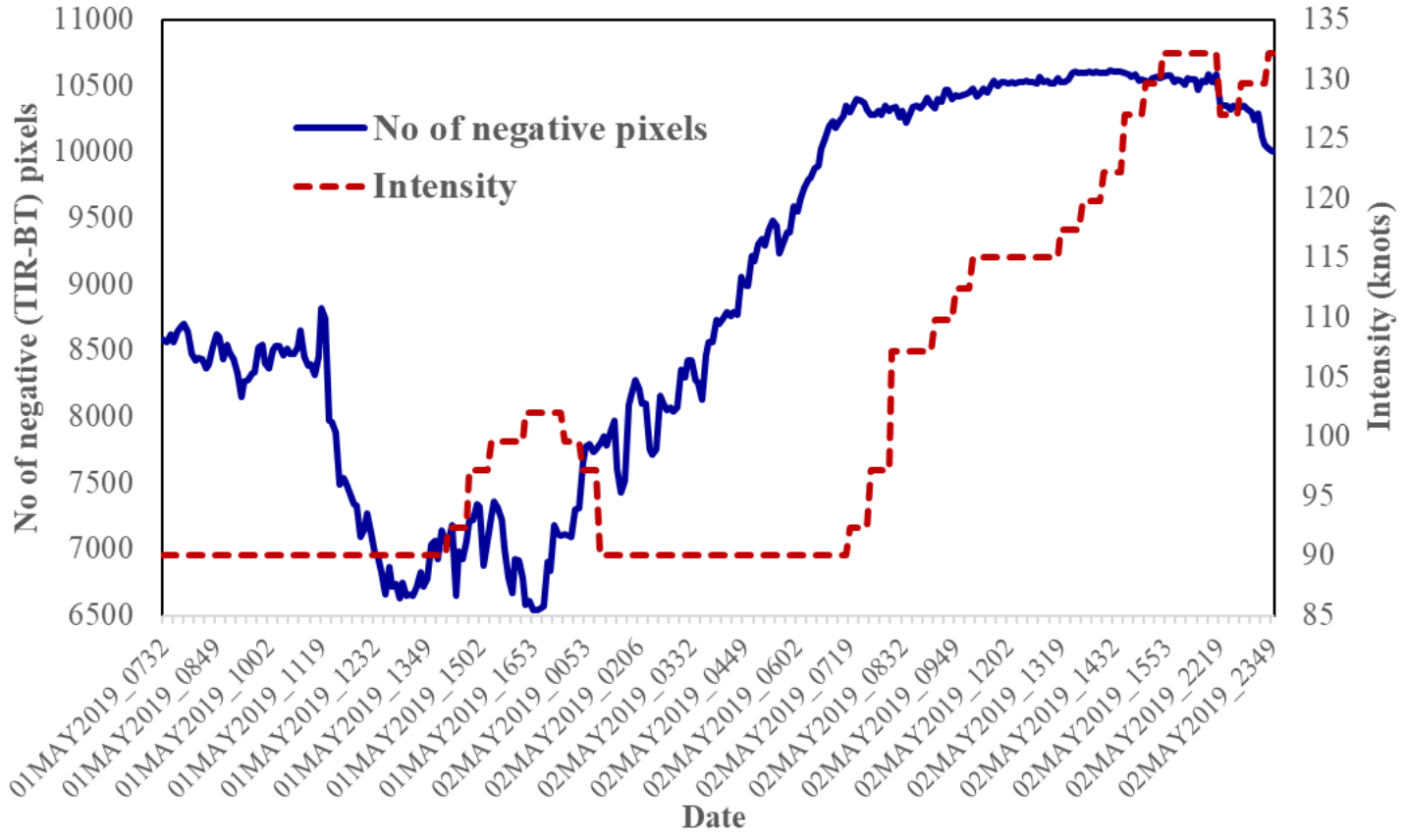

Figure 8

The time series plot of number of negative TIR1-WV pivels in TC inner core region and intensity

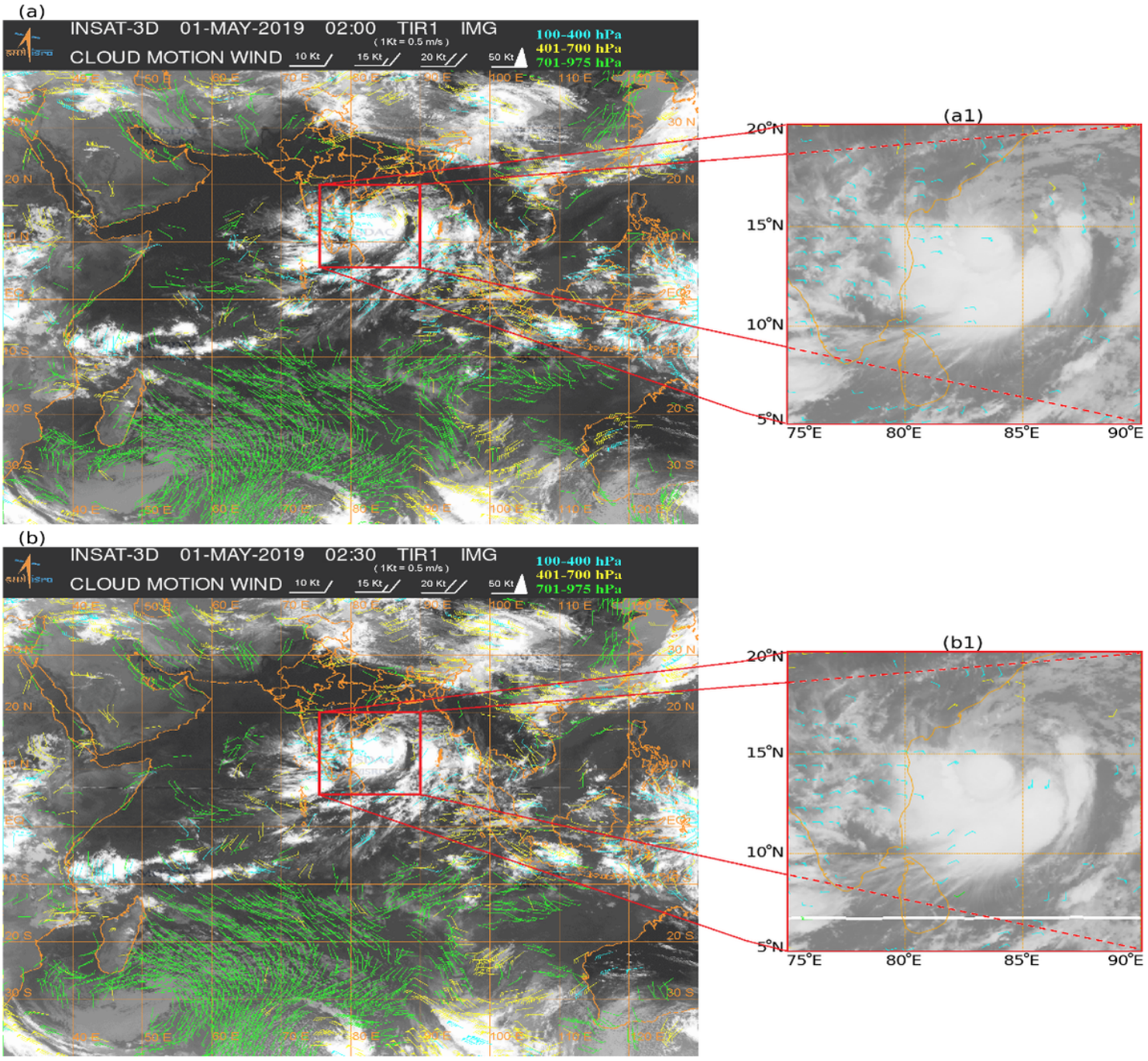

Figure 9

Atmospheric motion winds generated using INSAT-3D infrared 30-minute images valid at (a) 0200 UTC and (b) 0230 UTC 01 May, 2019

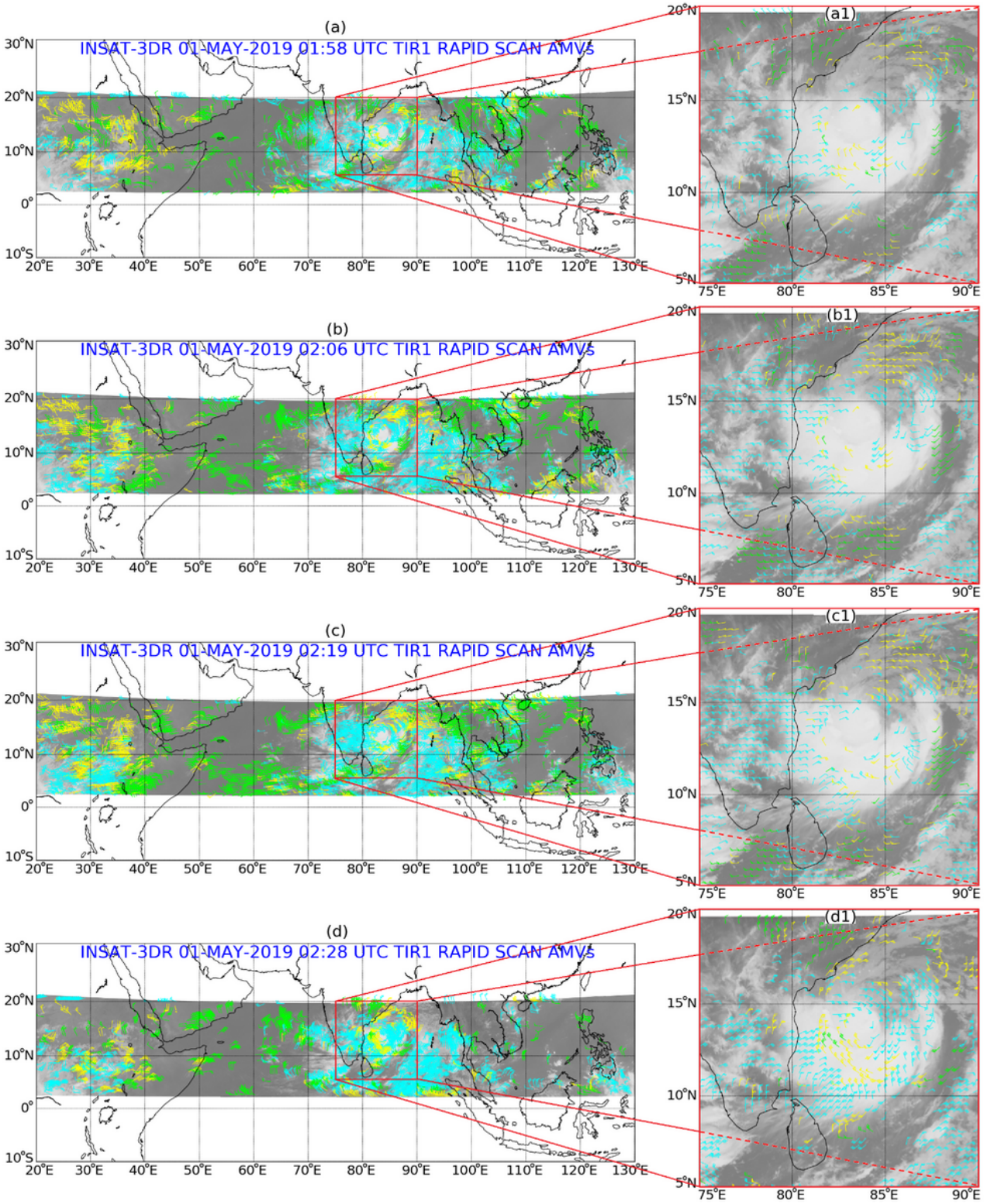

Figure 10

Rapid scan winds generated using INSAT-3DR infrared images over Indian Ocean region valid at: a) 0158 UTC, b) 0206 UTC, c) 0219 UTC and d) 0228 UTC of 01 May, 2019.

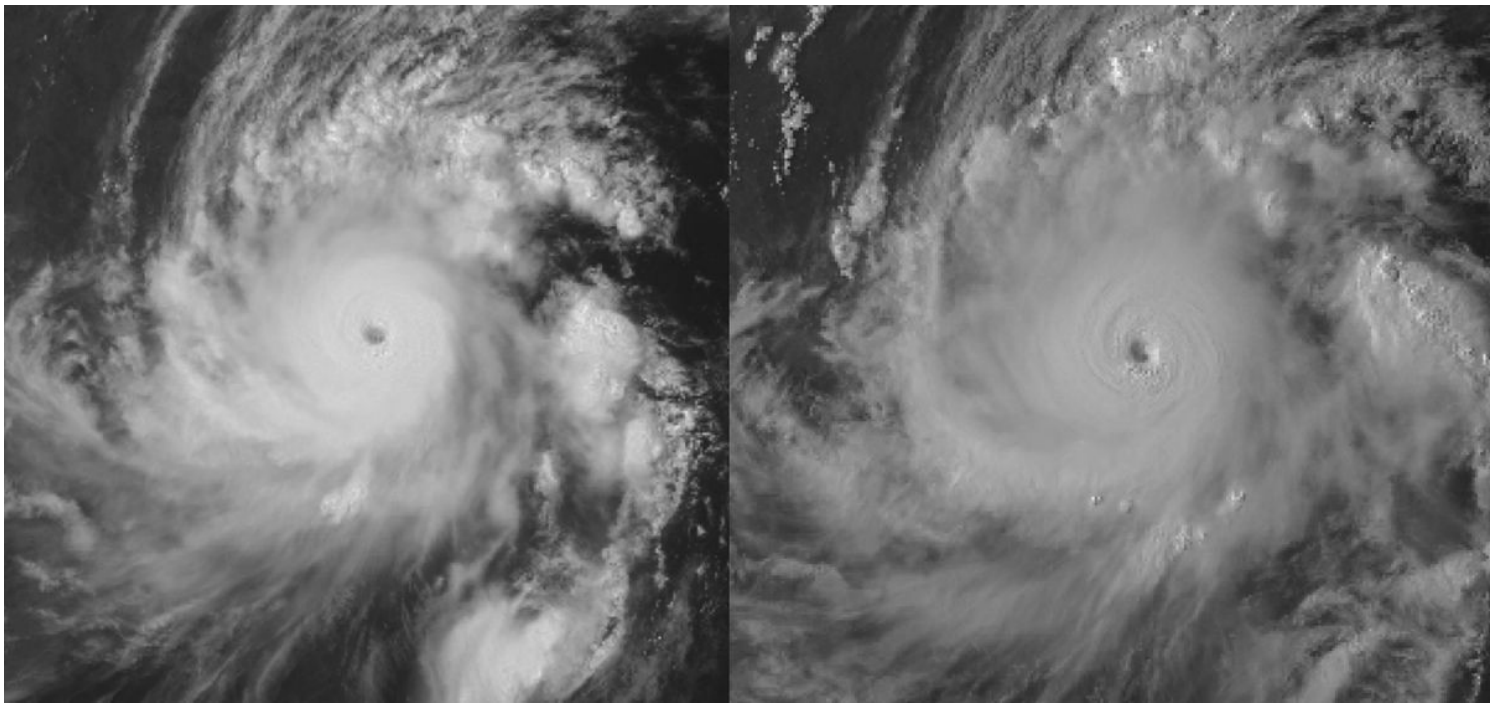

Figure 11

visible wavelength satellite view of TC FANI during its peak intensity stage at 0802 UTC (left) and 0945 UTC (right) 02 May 2019.

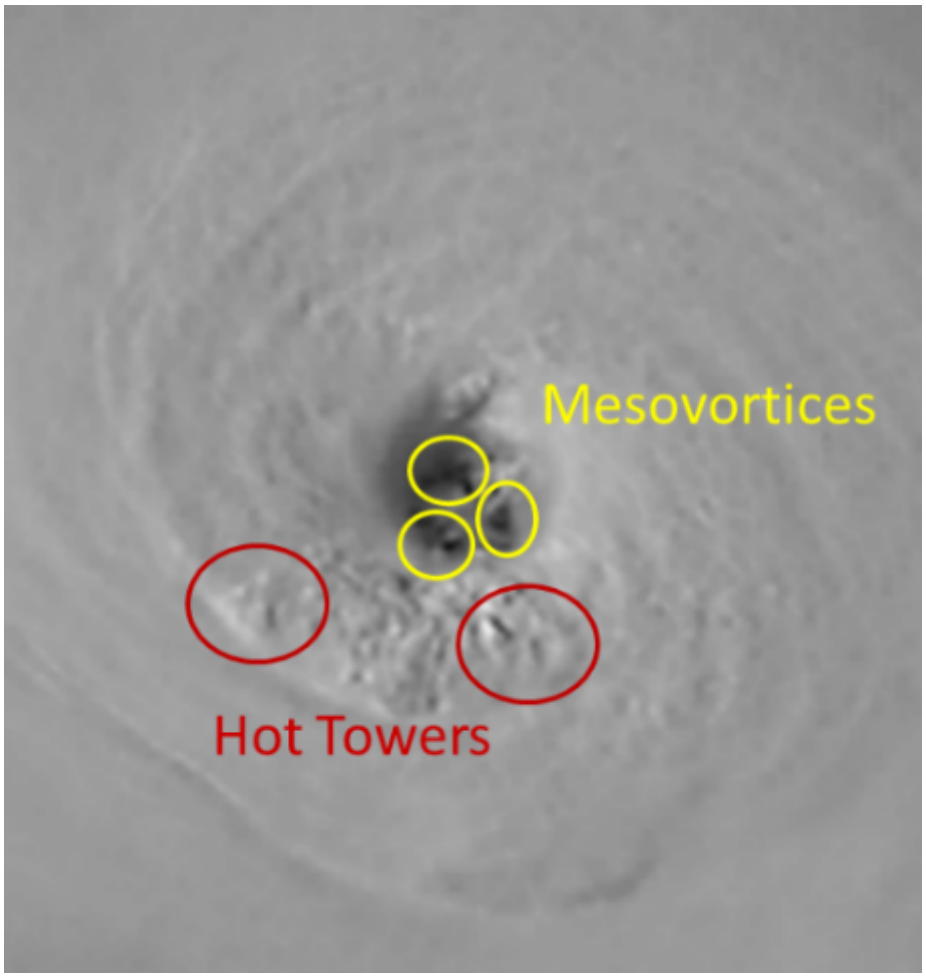

Figure 12

The low-level mesovortices and hot towers depicted by the INSAT-3DR visible channel image at 0906 UTC 02 May 2019.

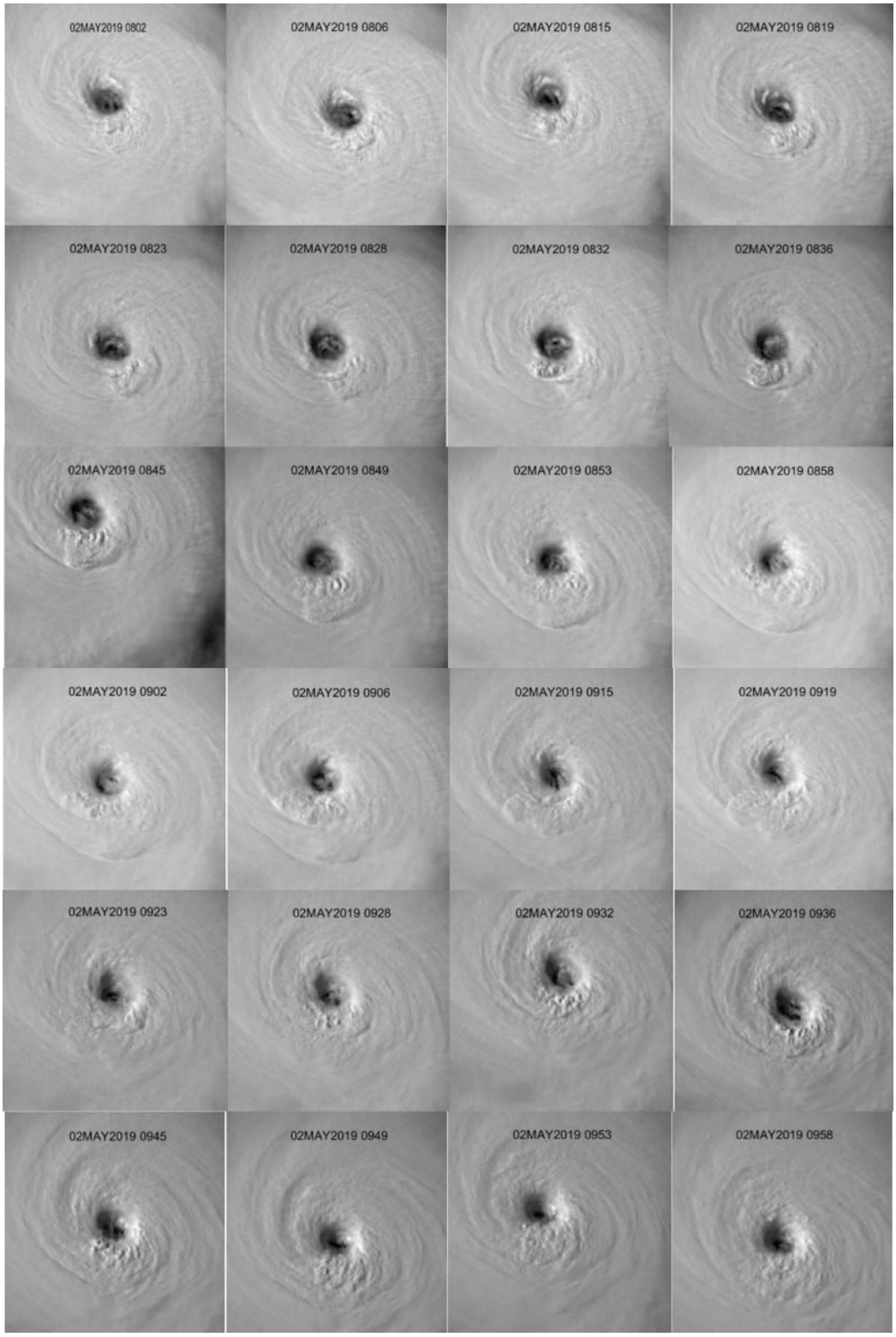

Figure 13

INSAT-3DR visible channel images of Eye of TC FANI during 0802-0958 UTC 02 May 2019.

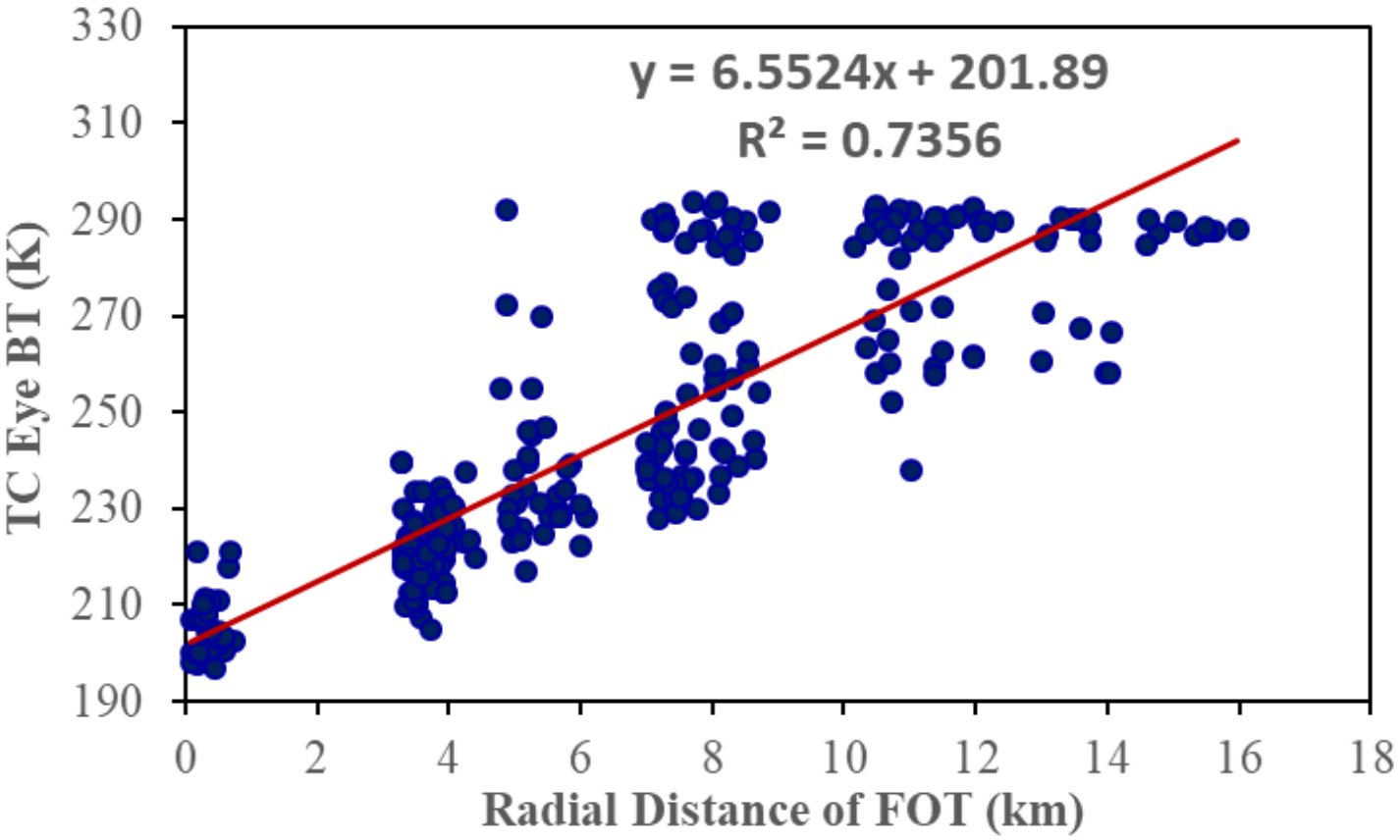

Figure 14

Scatter plot between radial distances of first overshooting top (FOT) and TIR1 BT of TC eye.

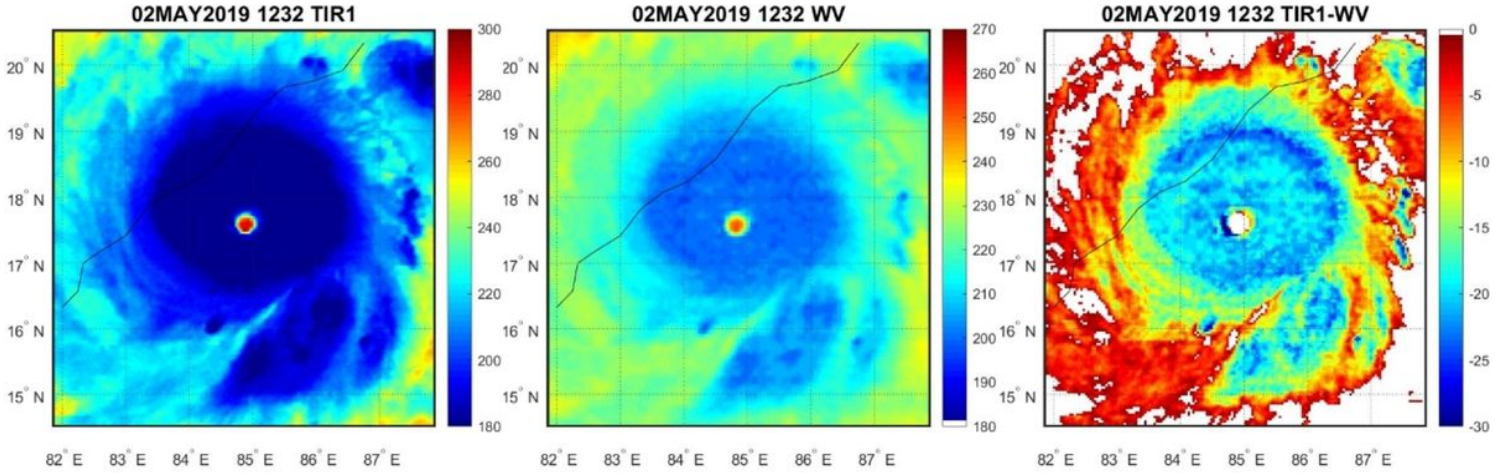

Figure 15

The inner core of TC observed by TIR1, WV and differenced TIR1-WV channels during its warmest eye condition.

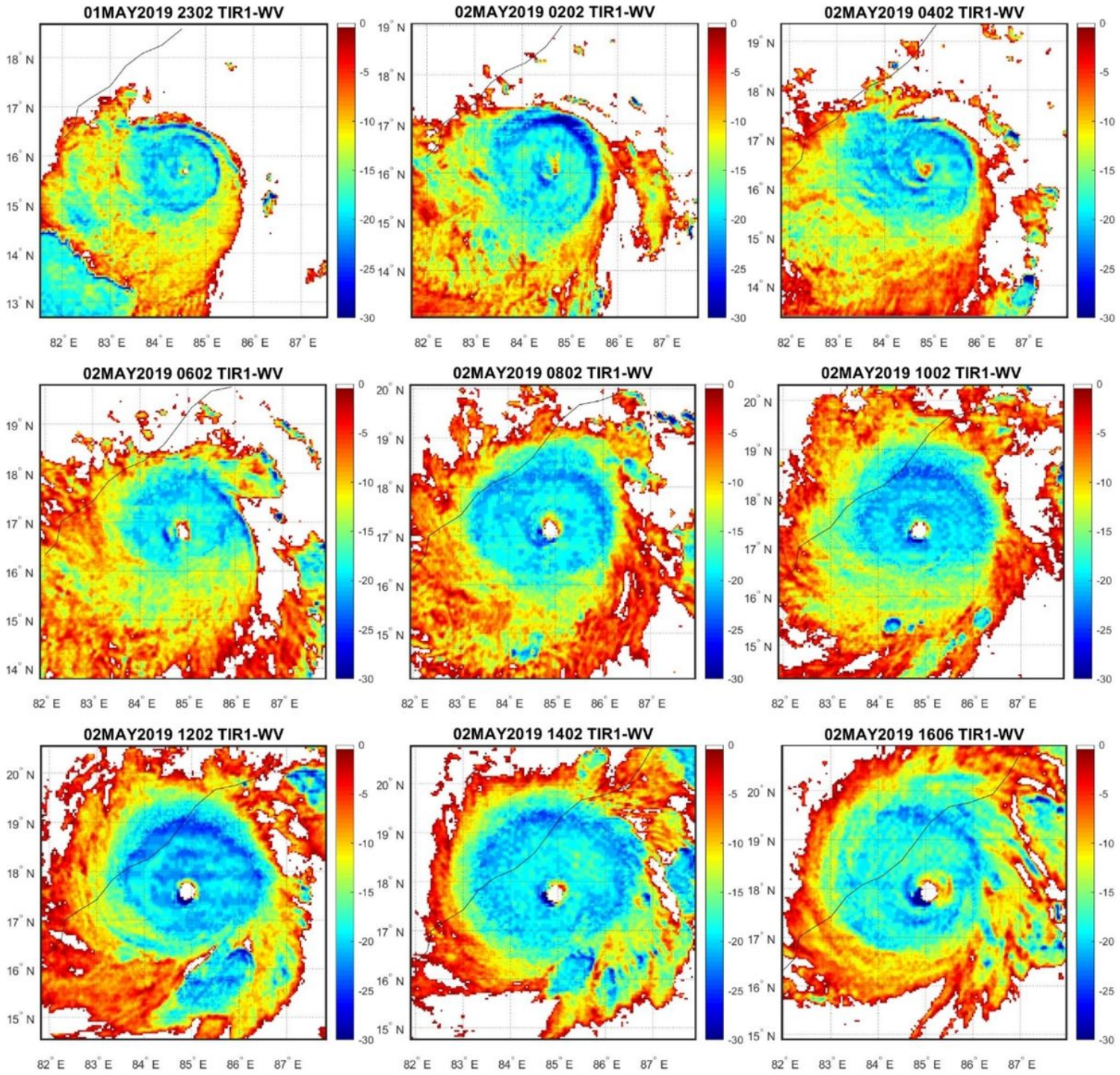

Figure 16

TIR-WV BT representing increasing FOT during TC intensification